Pertanika J. Sci. & Technol. 31 (5): 2389 - 2412 (2023)

PERTANIKA JOURNALS

SCIENCE & TECHNOLOGY

Journal homepage: http://www.pertanika.upm.edu.my/

A Study on Bio-Stabilisation of Sub-Standard Soil by Indigenous Soil Urease-Producing Bacteria

Abdulaziz Dardau Aliyu[1,2], Muskhazli Mustafa[1]*, Nor Azwady Abd Aziz[1] and Najaatu Shehu Hadi[1]

[1]Department of Biology, Faculty of Science, Universiti Putra Malaysia, 43400 UPM, Serdang, Selangor, Malaysia
[2]Department of Microbiology, Faculty of Science, Federal University of Lafia, Akunza 950101, Nasarawa State, Nigeria

ABSTRACT

Sub-standard soils are of great concern worldwide due to diverse economic losses and the possibility of severe environmental hazards ranging from catastrophic landslides, building collapse, and erosion to loss of lives and properties. This study explored the potential of urease-producing bacteria, *Bacillus cereus* and *Bacillus paramycoides,* to stabilise sub-standard soil bio-stabilisation. The maximum urease activity measured by *B. cereus* and *B. paramycoides* was 665 U/mL and 620 U/mL, respectively. *B. cereus* and *B. paramycoides* precipitated 943 ± 57 mg/L and 793 ± 51 mg/L of $CaCO_3$ at an optical density (425 nm) of 1.01 and 1.09 and pH 8.83 and 8.59, respectively, after 96 hours of incubation. SEM microstructural analysis of the precipitated $CaCO_3$ revealed crystals of various sizes (2.0–23.0 µm) with different morphologies. XRD analysis confirmed that the precipitated $CaCO_3$ comprised calcite and aragonite crystals. SEM analysis of the microstructure of organic and sandy clay soils treated with *B. cereus* and *B. paramycoides* showed the formation of bio-precipitated calcium carbonate deposits on the soil particles (biocementing soil grains), with *B. cereus* precipitating more $CaCO_3$ crystals with a better biocementing effect compared to *B. paramycoides*. Overall, the experimental results attributed $CaCO_3$ formation to bacterial-associated processes, suggesting that soil ureolytic bacteria are potentially useful to stabilise sub-standard soil.

Keywords: Bio-stabilisation, calcite, calcium carbonate, micp, urease enzyme, ureolysis

ARTICLE INFO

Article history:
Received: 15 August 2022
Accepted: 25 January 2023
Published: 21 July 2023

DOI: https://doi.org/10.47836/pjst.31.5.18

E-mail addresses:
aliyuabdulaziz23@gmail.com (Abdulaziz Dardau Aliyu)
muskhazli@upm.edu.my (Muskhazli Mustafa)
azwady@upm.edu.my (Nor Azwady Abd Aziz)
Shehuhadinajaatu@gmail.com (Najaatu Shehu Hadi)
*Corresponding author

ISSN: 0128-7680
e-ISSN: 2231-8526

INTRODUCTION

There is a high demand for land for civil infrastructure, particularly in urban areas, due to rapid population growth in both developing and developed nations (Sinha & Chattopadhyay, 2016). On the contrary, landmass for various construction purposes continues to become relatively scarce (Bernardi et al., 2014). This rapid growth enhances the high demand for land utilisation to meet various basic human needs, necessitating infrastructural development on sub-standard soils (Chang et al., 2016). Geotechnical engineers define a sub-standard soil type as having inferior engineering features and cannot be effectively utilised for construction without an improvement technique (Rabenhorst et al., 2020). Indeed, there is an estimated global financial loss of up to seven billion US dollars annually due to the failure of various geotechnical structures built on sub-standard soils (Singh et al., 2020).

In Malaysia, the Department of Environment reported that 2.56 million hectares of land (representing 7.74%) are covered with sub-standard peat soils, mostly distributed within Sarawak (1,697,847 hectares) and Selangor (164,708 hectares) states (Wahab et al., 2019; Sapar et al., 2020). Furthermore, during the last two decades, there have been more than 400 landslides comprising over 30 major landslides involving both natural and cut slopes, which have destroyed properties worth billions of ringgits and claimed over 200 lives due to the high compressibility and low shear strength of these tropical peatland sub-standard soils (Makinda et al., 2018). The poor soil characteristics may affect the foundations of multi-storey buildings, pavements, retaining walls and dams with devastating consequences such as slip failures, local sinking and massive settlements. Thus, an urgent need is to develop an effective, less evasive, durable and relatively environment-friendly soil stabilisation method.

Despite the numerous advances in using conventional materials and methods for soil stabilisation, challenges remain to overcome (Nawarathna et al., 2018). Industrial manufacturing of mineral additives such as cement has economic and environmental concerns, such as high energy consumption and CO_2 emission accounting for 7% of the world's anthropogenic emissions (Nawarathna et al., 2018; Nething et al., 2020), which contributes to climate change (Wong, 2015). An alternative method to stabilise sub-standard soil is microbial urease enzyme technology known as Microbially Induced Calcite Precipitation (MICP).

MICP utilises eco-friendly features of urease-producing bacteria to hydrolyse urea (ureolysis) in a series of complex biochemical reactions to generate ammonium and carbonate ions. The ammonium ions favour precipitation by increasing the pH (Terzis & Laloui, 2019; Filet et al., 2020). The bacteria cell surface has a net negative charge as a negative zeta potential (Renner & Weibel, 2011), thus providing binding sites for carbonate

ions with available divalent calcium ions within the micro-environment under sufficient supersaturation conditions, hence precipitating cementitious calcite crystals on the cell surface (Dardau et al., 2021). These precipitated inorganic carbonate crystals further cement soil grains together, filling inter-particle voids, thereby improving the physical and mechanical properties of sub-standard soils (Lutfian et al., 2020). The success of the MICP process is promoted primarily by *in situ* conditions such as particle size and distribution, temperature, water content and treatment conditions like cementation solution and bacterial concentrations (Dadda et al., 2018).

MICP is considered one of the most effective soil stabilisation technologies (Ghosh et al., 2019; Ivanov et al., 2020), thus, has the potential to address a wide range of geoenvironmental and geotechnical issues (Miftah et al., 2020), including erosion control in coastal areas, enhancing the stability of non-piled and piled foundations, pavement surface treatment, reducing dust levels on exposed loose soil surfaces by binding the dust particles together, and reinforcing soil to improve underground constructions (Wath & Pusadkar, 2016). Furthermore, the technique can also be applied to various soil types ranging from coarse and well-graded sands to finer soils, but it is more effective for coarse and well-graded sands (Mortensen et al., 2011). Although previous literature presented encouraging and impressive results on the stabilisation of sub-standard soils via exogenous ureolytic bacterial strains procured commercially from microbial culturing centres (Jain & Arnapalli, 2019; Hoang et al., 2019), the introduction of such strains to the soil environment may adversely disturb the natural eco-system balance (indigenous bacterial strains present).

Furthermore, bacterial cultivation, special precautions required during mixing, the survivability of the exogenous bacteria and the long time required for the permeation of the bacteria render this process costly, thus challenging for large-scale implementation (Tiwari et al., 2021). However, very limited studies focus on the potential of indigenous ureolytic bacterial strains distributed within the soil (Bibi et al., 2018). Hence, this study focuses on the potential of indigenous soil urease-producing bacterial strains to reduce costs.

This study focused on the potential MICP treatment of organic and sandy clay soils by indigenous ureolytic bacteria. It is also the first study involving the application of MICP using indigenous *B. paramycoides* for sub-standard soil stabilisation. The maximum urease activity of *B. cereus* and *B. paramycoides* were measured, and the bio-precipitated $CaCO_3$ crystals were evaluated to prove the biocementing effect of both bacterial species as potential MICP agents to stabilise sandy clay and organic soils. The study outcomes are expected to serve as a reference for an improved, simple natural bio-mediated soil stabilisation method via the precipitation of calcium carbonate by ureolytic bacteria.

MATERIALS AND METHODS

Bacterial Culture

Two bacterial species, *Bacillus cereus* (https://www.ncbi.nlm.nih.gov/nuccore/NR_115714.1) and *Bacillus paramycoides* (https://www.ncbi.nlm.nih.gov/nuccore/NR_157734.1) were isolated from sub-standard soil on a farm at Universiti Putra Malaysia in Selangor, Malaysia. The bacterial species stocks were maintained in sterilised microcentrifuge tubes at -82°C in 30% sterile glycerol, and the bacterial cells were activated by cultivation on calcium carbonate precipitation agar containing 10 g/L NH_4Cl, 3 g/L nutrient agar, 20 g/L agar, 20 g/L urea and 2.12 g/L $NaHCO_3$ for 24 hr at 28 ± 0.5°C before use (Wei et al., 2015; Bibi et al., 2018).

Urease Activity

The urease activity was quantified by the phenol hypochlorite assay as previously described by Chahal et al. (2011). The mixture was measured at an optical density of 626 nm, and ammonium chloride (50 to 100 µM) was used as a standard, with one unit of urease defined as the amount of enzyme hydrolysing 1 µmol urea/minute.

Quantification of Precipitated Crystals

The method adapted from Wei et al. (2015) was used to quantify the precipitated carbonate crystals produced by *B. cereus* and *B. paramycoides*. The bacterial isolates were grown in 100 mL of calcium carbonate precipitation (CCP) broth and incubated for 96 hr at 28 ± 0.5°C, with an uninoculated CCP medium used as a control. After incubation, the bacterial cultures were centrifuged at 4,000 g for 4 min. The pellet containing precipitated $CaCO_3$ and the ureolytic bacteria cells were resuspended in 50 mL TE buffer (pH 8.5, 10 mM Tris, 1 mM EDTA) before 1 mg/mL lysozyme was added and incubated for 60 min at 37 ± 0.5°C to break down the ureolytic bacteria cell walls. The suspension was centrifuged to remove cell debris, and the pellet was washed with distilled water (pH 8.5), then air dried for 48 hr at 40 ± 0.5°C and weighed to quantify the precipitated carbonate crystals. The quick acid test, according to the method by Richardson et al. (2014), was then performed to confirm the formation of carbonate crystals. The precipitated carbonate crystals were placed in dried sterile test tubes before the dropwise addition of 10% (v/v) of hydrogen chloride. The rapid effervescence with bubble formation confirmed carbonate crystals.

Characterisation of the Precipitated Crystals

The $CaCO_3$ crystals were characterised by a scanning electron microscope (SEM) and X-ray diffraction (XRD) (Dhami et al., 2016; Liu et al., 2017). The samples were crushed to evenly distribute the particles before mounting them on the stub. The sample was then

gold sputtered (BAL - TEC SCD 005, Williston, USA) for 3 min to increase conductivity, and the stub was mounted onto the JSM–IT100 InTouch Scope ™ (Tokyo, Japan). The XRD spectra of the crushed dried samples were obtained using Shimadzu 6000 Diffractometer (Kyoto, Japan) to identify the crystalline phase composition and crystalline nature (calcite, vaterite, aragonite or amorphous calcium carbonate crystals). The samples were scanned at 2.00 (deg/min) from 20.00 – 70.00 2Θ with the Cu anode at 30 kV and 30 mA.

Analysis of the Role of Ureolytic Bacteria in MICP

The texture of the treated soil samples was determined as described by Towner (1974) and Ritchey et al. (2015), while the potential deposition of carbonate crystals by *B. cereus* and *B. paramycoides* to stabilise sandy clay soil and organic soil was studied based on the previously described method by Bibi et al. (2018). Approximately 50 mL cultures of urea medium containing 0.6 g of soil, 20 g/L of urea and 3.7 g/L of $CaCl_2.2H_2O$ was used to inoculate ureolytic bacterial isolates with an initial concentration of 0.1 at an optical density of 600 nm. The culture was incubated at 28 ± 0.5°C at 120 rpm for 30 days on a controlled temperature incubator shaker (Infors Ecotron, Bottmingen, Switzerland). Ten experimental setups in triplicates were prepared, as shown in Table 1. *B. cereus* and *B. paramycoides* were cultured in tests A, B and C, D, respectively. On the 30th day, treated samples were washed three times with distilled water, and the pellets were oven dried at 40 ± 0.5°C for 48 hr. Dried-treated soil samples were analysed using SEM and XRD to confirm $CaCO_3$ (Dhami et al., 2016; Liu et al., 2017).

Table 1

The experimental setup for analysis of ureolytic bacteria's role in calcite precipitation

Test	Medium	Soil type	Isolate
A	Urea + $CaCl_2.2H_2O$	Sandy clay soil	*Bacillus cereus*
B	Urea + $CaCl_2.2H_2O$	Organic soil	*Bacillus cereus*
C	Urea + $CaCl_2.2H_2O$	Sandy clay soil	*Bacillus paramycoides*
D	Urea + $CaCl_2.2H_2O$	Organic soil	*Bacillus paramycoides*
E	Urea + $CaCl_2.2H_2O$	Organic soil	-
F	Urea + $CaCl_2.2H_2O$	-	-
G	Urea	Sandy clay soil	-
H	Urea	Organic soil	-
I	Distilled water	Sandy clay soil	-
J	Distilled water	Organic soil	-
K	Distilled water	-	-

RESULTS AND DISCUSSION

Bacterial Culture and Measurement of Urease Activity

There are diverse bacterial species inhabiting the soil, among which ureolytic bacteria are particularly abundant (Hasan, 2000; Oshiki et al., 2018). In the present study, *B. cereus* and *B. paramycoides* were isolated from farm soils, as such soils are rich in urea due to the frequent use of organic manure and synthetic urea fertilisers, which improve microbial activity through stimulating *in situ* urease-producing bacteria within the soil pores (Zhu & Dittrich, 2016). Farm soils contain urea for urease-producing bacteria to utilise as sole nitrogen and energy sources, thus, enhancing the rapid distribution, diversity and adaptability of these microbes within the soil environment (San Pablo et al., 2020; Svane et al., 2020).

As shown in Figure 1, there was a steady increase in *B. cereus* and *B. paramycoides* urease activity with incubation time reaching a maximum urease activity of 665 U/mL and 620 U/mL, respectively, indicating their suitability as potential agents for MICP soil stabilisation. By comparison, the study by Chahal et al. (2011) reported unidentified soil ureolytic bacterial isolates with maximum urease activity of 598 U/mL, 593 U/mL and 589 U/mL, respectively. Similarly, Li et al. (2015) reported *that B. megaterium* recorded maximum urease activity of 592 U/mL after 120 hr incubation. According to the study, *B. megaterium* increases the unconfined compressive strength of the urease-based treated sand sample to 1002 KPa with a decrease in permeability to 2.0 x 10^{-7} ms^{-1} due to the high urease activity recorded. The steady decrease in urease activity observed in this study after 96 hr and 120 hr is probably due to cell death, metabolism inhibition, exhaustion of nutrients, and enzyme degradation with time, leading to an irreversible loss of urease activity (Jiang et al., 2016). Sub-standard soil stabilisation via MICP is initiated by the microbial enzyme urease, which catalyses urea decomposition (Bzura & Koncki, 2019), consequently increasing the pH and production of inorganic mineral carbonate crystals, such as calcite (Omoregie et al., 2019; Jiang et al., 2020).

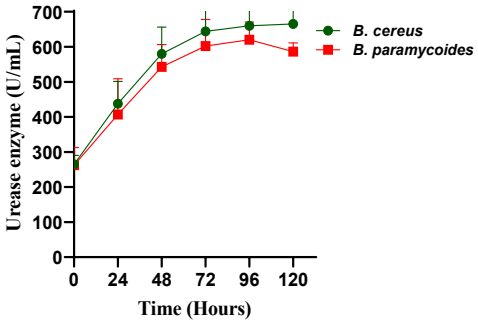

Figure 1. Urease activity (optical density 626 nm) of *B. cereus* and *B. paramycoides*. Error bars represent the standard deviation of the mean

Quantification of Precipitated Crystals

Individual ureolytic bacterial strains have different urease production rates, influencing the amount of $CaCO_3$ precipitated (Qabany et al., 2011). Thus, it becomes paramount to determine the amount of $CaCO_3$ produced by the ureolytic bacteria to evaluate its calcifying potential. Therefore, the $CaCO_3$

precipitated at 96 hr incubation time by *B. cereus* and *B. paramycoides* was quantified and studied in relation to cell growth (Figure 2) and pH (Figure 3). As observed from Figure 2, the amount of $CaCO_3$ precipitated by *B. cereus* and *B. paramycoides* were 655 mg/L and 546 mg/L at a bacterial growth of 0.83 and 0.76 at the optical density of 425 nm within 48 hr, respectively, while at 96 hr, the precipitated $CaCO_3$ increased to 943 mg/L and 793 mg/L with a corresponding increase in bacterial growth to 1.01 and 1.09 respectively.

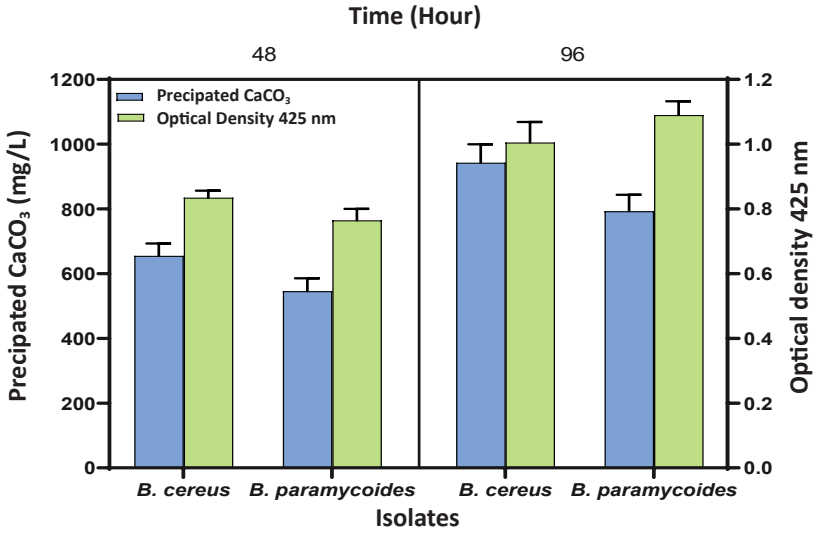

Figure 2. Comparison of the bacterial growth and potential of calcium carbonate precipitation among *B. cereus* and *B. paramycoides*. Error bars represent the standard deviation of the mean.

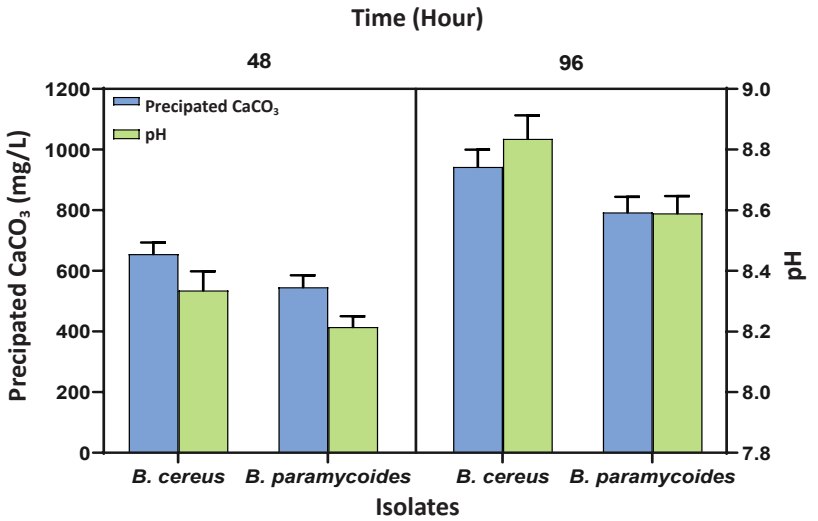

Figure 3. Comparison of the pH and potential of calcium carbonate precipitation among *B. cereus* and *B. paramycoides*. Error bars represent the standard deviation of the mean.

Although both isolates recorded an increase in precipitation with time, *B. cereus* precipitated more $CaCO_3$ than *B. paramycoides*. Further, most of the precipitated $CaCO_3$ by both isolates was produced within the first 48 hr, in contrast to the study of Kim et al. (2018), which reported that most calcite precipitation by *Staphylococcus saprophyticus* and *Sporosarcina pasteurii* occurred within 72 hr. This study adopted a 96 hr incubation based on the maximum precipitation period achieved by both bacteria. Wei et al. (2015) reported that *B. lentus*, *B. diminuta* and *S. soli* precipitated 931 mg/L, 842 mg/L and 456 mg/L of $CaCO_3$. Noteworthy, findings from previous reports and the current study reveal that individual ureolytic bacterial species precipitated different amounts of $CaCO_3$ despite being incubated under similar growth and cultural conditions (Wei et al., 2015; Kim & Youn, 2016; Kim et al., 2018). This variation in the quantity of $CaCO_3$ crystals precipitated across individual ureolytic bacterial species might be due to individual differences in bacterial urease activity, favouring CO_3^{2-} concentrations generated during urea breakdown and resulting in differences in $CaCO_3$ precipitation. Thus, the higher precipitation achieved by *B. cereus* compared to *B. paramycoides* in this study was expected based on the highest urease activity recorded (Figure 1), which was in relatively good agreement with the amount of calcium carbonate precipitated (Figure 2).

The increased $CaCO_3$ precipitation by both isolates corresponds to an individual increase in bacterial growth with increasing incubation over 96 hr. Further, *B. paramycoides* grew faster after 48 hr recording higher bacterial growth of 1.09 after 96 hr but precipitated less $CaCO_3$ than *B. cereus*. It implies that higher bacterial cell growth may not correspond to higher urease activity which does not necessarily translate to a higher $CaCO_3$ yield (Bibi et al., 2018) because urease activity is the main factor favouring a higher $CaCO_3$ yield during MICP (Mwandira et al., 2019; Tang et al., 2020).

Optimum proteolysis occurs at a pH favouring bacterial growth and metabolism, and the pH of the bacterial medium plays a significant role in inducing microbial morphological changes, affecting its stability and instigating enzyme secretion (Omoregie et al., 2017). Urea hydrolysis occurs due to the secretion of urease by the bacteria, which generates carbonate ions precipitated as $CaCO_3$ crystals (Wu et al., 2017). As shown in Figure 3, *B. cereus* and *B. paramycoides* increased the medium pH to 8.33 and 8.21, respectively, after 48 h, indicating that both isolates require an alkaline pH for maximum $CaCO_3$ precipitation. The medium alkaline pH enhances the physiological conditions favourable for the ureolytic bacterial cell wall acting as the nucleation site for mass $CaCO_3$ precipitation (Imran et al., 2019). After 96 hr, the $CaCO_3$ precipitation reached a plateau pH of 8.83 and 8.59, respectively, implying that $CaCO_3$ precipitation corresponds with an increase in pH over the incubation period, and this has been well documented in several studies (Park et al., 2010; Keykha et al., 2017). The steady increase in pH may enhance the transportation of growth factors and other essential nutrients across the bacterial cell membrane, probably

by facilitating active transport or diffusion (Wiley & Stokes, 1963; Morsdorf & Kaltwasser, 1989), favouring mass $CaCO_3$ precipitation which enhances the MICP treatment of sub-standard soils (Wu et al., 2017).

By comparison, Kim et al. (2018) reported maximum $CaCO_3$ precipitation by *Staphylococcus saprophyticus* and *S. pasteurii* at pH 7.0, and Wei et al. (2015) reported a pH of 9.6 for *B. lentus.* It implies that individual ureolytic bacteria have their unique peak pH favouring maximum calcite precipitation, which varies from neutral to an alkaline pH.

Characterisation of the Precipitated Crystals

Precipitated $CaCO_3$ by both *B. cereus* and *B. paramycoides* was confirmed by a quick acid test (Figure 4) (Richardson et al., 2014). $CaCO_3$ precipitated by *B. cereus* was visualised under a light microscope showing that some rhombohedral crystals formed aggregates, as shown in Figure 4a, while no precipitates were formed in the uninoculated medium. These precipitates were formed by supersaturation within the medium, with the bacterial cell wall acting as nucleation sites (Wang et al., 2017). The morphology of the $CaCO_3$ crystals observed in this study was relatively similar to the rhombohedral $CaCO_3$ crystals previously observed in aggregates, as reported by the study of Al-Thawadi and Cord-Ruwisch (2012). Noteworthy, in the present study, only calcite crystals were visualised under the light microscope, justifying further adaptation of the SEM-XRD technique for a more detailed microstructural analysis which confirmed the presence of aragonite crystals.

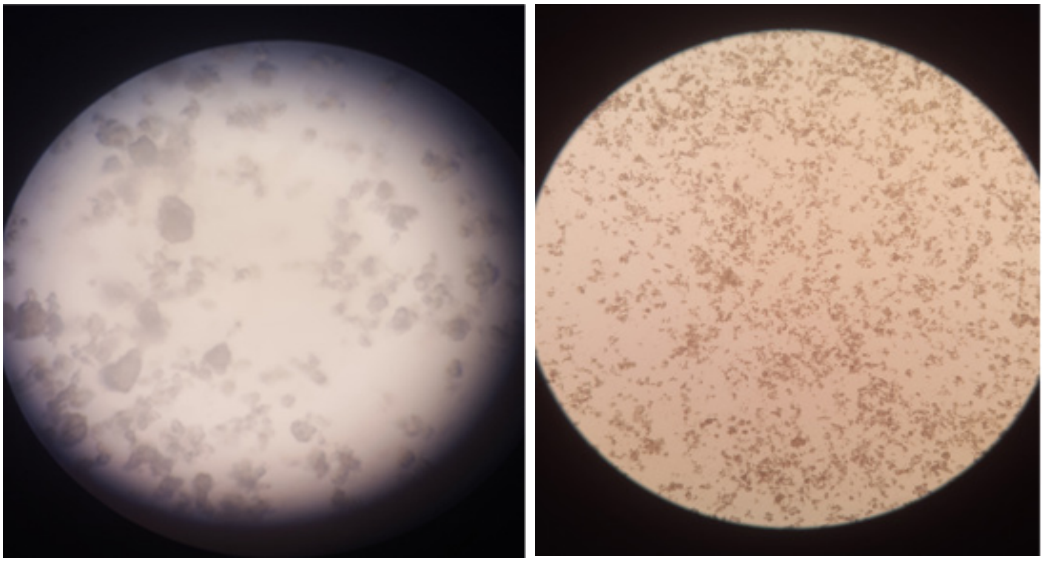

(a) (b)

Figure 4. Microscopic images of precipitated calcium carbonates viewed under Light microscope (a) *Bacillus cereus* (b) *Bacillus paramycoides*.

The XRD spectra of *B. cereus* precipitated $CaCO_3$ (Figure 5a) showed distinct peaks at 23.2°, 29.6°, 36.1°, 39.6°, 48.6°, 57.5°, 60.8° and 64.8° attributed to the typical calcite structure abundantly precipitated with aragonite identified at 2theta diffraction angle of 43.3°. Further, *B. paramycoides* $CaCO_3$ XRD spectra (Figure 5b) showed characteristic diffraction peaks at an angle of 29.6°, 36.2°, 39.6°, 48.7° and 57.6°, 60.8°, revealing that the most precipitated bio-product was calcite. In comparison, only a 2theta diffraction angle of 43.3° was identified as aragonite. Therefore, calcite crystals were the most abundant precipitated $CaCO_3$ polymorph by both *B. cereus* and *B. paramycoides*.

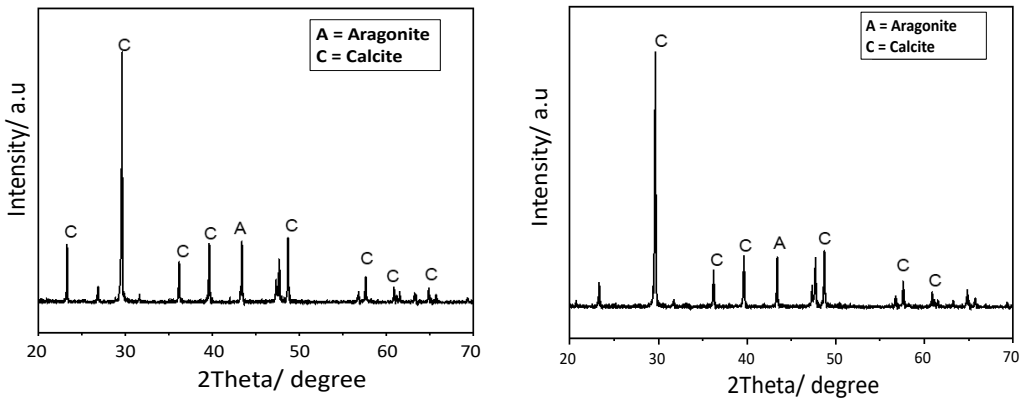

Figure 5. XRD spectra of precipitated calcium carbonate crystals by (a) *B. cereus* and (b) *B. paramycoides*

The *B. cereus* precipitated calcite minerals of different morphology comprised clustered rhombohedral crystals, cubic crystals of roughly similar sizes and a few irregular calcite crystals (Figure 6 a-c). Other crystals were also observed, like flower-shaped calcite up to 8.0 µm in diameter (Figure 6c). The findings from this study were consistent with previous observations by Wei et al. (2015), Oral and Ercan (2018) and Wen et al. (2020). The irregular calcite crystals were amorphous with several tiny holes on the surface (2.7–3.4 µm). By contrast, Luo and Qian (2016) observed larger irregular calcite crystals of 50 µm diameter. Furthermore, the cubic crystals have smooth surfaces ranging from 2.0 to 2.7 µm. On the contrary, Zhang et al. (2019) reported larger irregular cubic crystals (53.4 µm). Irregular cubic and spherical crystals favour better soil biocementation (Tang et al., 2020).

In contrast, the precipitated mineral induced by *B. paramycoides* was composed mainly of irregular calcite particles of different sizes (Figure 6f) and agglomerated rhomboids (Figure 6 d-e). The agglomerated rhombohedral calcite crystals were similar to those produced by *B. cereus* and similar to previous observations (Kakelar et al., 2016). Furthermore, the irregular calcite crystals (4.6–23.0 µm) induced by *B. paramycoides* had

a rough surface and were larger than the irregular calcite crystals (2.7–3.4 μm) precipitated by *B. cereus*.

The differences in $CaCO_3$ morphology are observed in numerous MICP processes and are usually influenced by several factors, such as differences in bacterial urease activity, which might be strain-specific (Kim & Lee, 2019), concentration and composition of the cementation solution, extracellular polymeric substances available on bacterial cell surfaces, rate of carbonation, CO_2 concentration, temperature and pH (Cizer et al., 2008; Tang et al., 2020). Various $CaCO_3$ crystal morphologies have been observed, including rhombic hexahedrons (Duo et al., 2018), ellipsoidal, spherical, rhombohedral (Dhami et al., 2013), flower-like, agglomerated rhomboids (Kakelar et al., 2016), lamellar rhombohedral (Zhang et al., 2019), irregular carbonate particles (Oral & Ercan, 2018), orthorhombic (Warren et al., 2001), hexagonal (Choi et al., 2017), framboidal aggregates (Mwandira et al., 2017), sponge-like (Srivastava et al., 2014) and capsule shape (Nawarathna et al., 2019).

Based on the SEM micrographs, no bacterial cells were visualised on crystals due to the lysozyme enzyme added to the medium after incubation, which breakdown all bacterial cell walls for clear differentiation of the crystals. By contrast, other authors observed bacterial cells embedded on similarly precipitated $CaCO_3$ crystals of different morphologies, as reported in this study. It demonstrated the direct involvement of the bacterial cell walls as nucleation sites for crystal formation (Bang et al., 2001; Duo et al., 2018). Interestingly, calcite formation from the recrystallisation of spherical vaterite crystals (2.9–5.3 μm) was partially observed in precipitated $CaCO_3$ by both *B. cereus* and *B. paramycoides* (Figure 6). It suggests that the calcite crystals were formed by the transformational disintegration and dissolution of earlier spherical vaterite crystals. Biocementation may commence with the initial formation of vaterite spherical crystals, which are meta-stable (Al-Thawadi & Cord-Ruwisch, 2012) but may gradually dissolve to recrystallise and form a more stable rhombohedral permanent calcite structure under a longer incubation period (Warren et al., 2001; Cheng et al., 2014).

However, the mechanism of rhombohedral crystal formation from spherical crystals remains unclear. Oral and Ercan (2018) observed the polymorphic transformation of vaterite to calcite with increased pH, indicating that this phenomenon might be related to supersaturation changes upon pH alteration. Kakelar et al. (2016) suggested that (1) vaterite crystals formation is kinetically favoured at higher urease activity, but when the urea is exhausted, there is a continuous decrease in urease activity, favouring calcite crystals formation and (2) the longer nucleation phase quickly decreases saturation which accelerates recrystallisation and dissolution, thus, favouring calcite abundance over vaterite. It may explain why no vaterite crystals were observed in the current study. Of note, factors influencing the polymorphic form of ureolytic bacterial $CaCO_3$ precipitation include the temperature of the solution, pH, precipitation time, degree of saturation, presence of

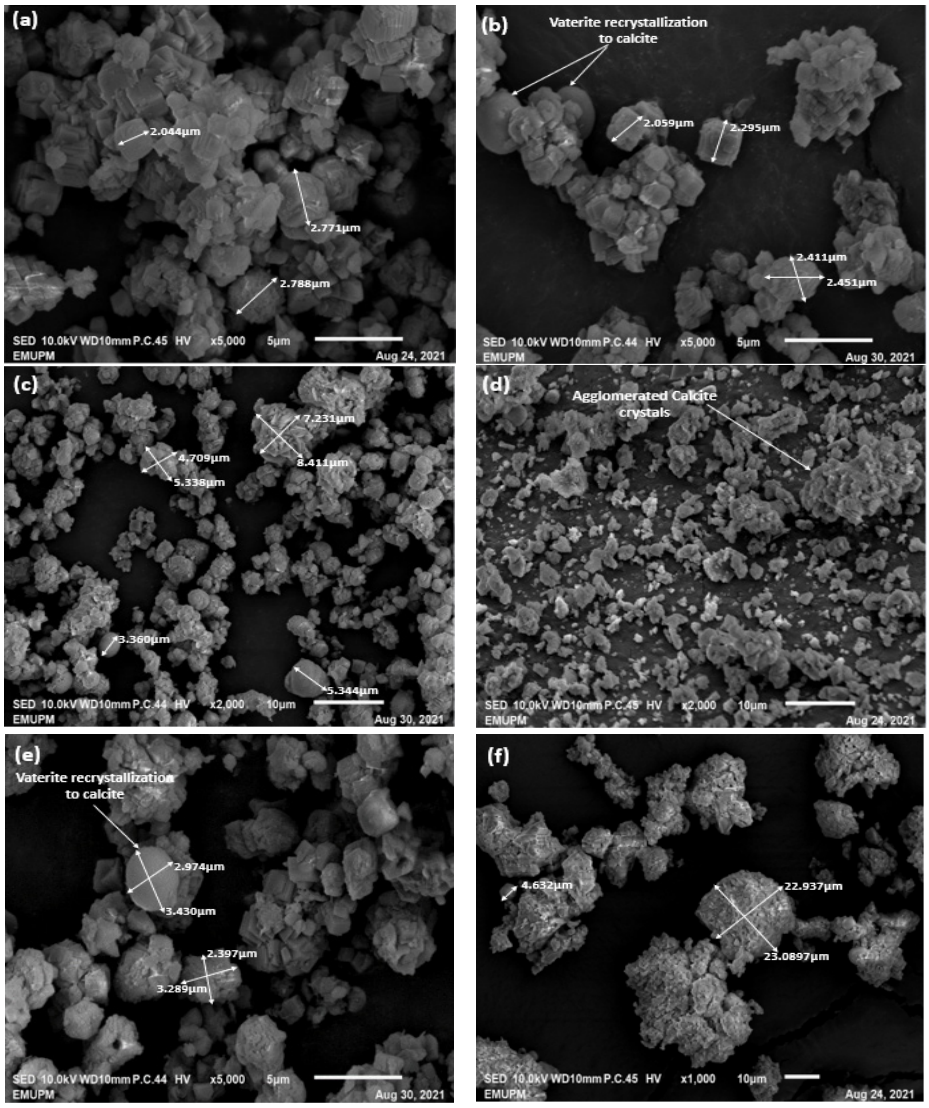

Figure 6. SEM micrographs showing different morphologies of precipitated calcium carbonate crystals by (a, b, c) *Bacillus cereus* and (d, e, f) *Bacillus paramycoides*

additives, the solvent used to dissolve precursors and stirring velocity (Oral & Ercan, 2018). In summary, the characterisation of $CaCO_3$ crystals induced by different ureolytic bacterial species favours the selection of the optimal species, thus, maximising the MICP efficiency. Further, photographs from SEM microanalysis have shown $CaCO_3$ crystals of different morphologies, confirmed by XRD to be mostly calcite precipitated by both *B. cereus* and *B. paramycoides*.

Analysis of the Role of Ureolytic Bacteria in MICP

Applying MICP to sub-standard soil will eventually result in the binding of the soil grains and the filling of inter-particle voids to stabilise the soil (Muthukkumaran & Shashank, 2016). In the current study, two soil types, sandy clay soil and organic soil, were treated with *B. cereus* and *B. paramycoides*. Figure 7 depicts treated organic and sandy clay soil by *B. cereus* formed flat, irregularly shaped solids of 24 mm and 22 mm in diameter, respectively; hence, indicating that *B. cereus* precipitated more $CaCO_3$ compared to *B. paramycoides*. Thus, consistent with previous results (Figure 2). It has been shown that larger $CaCO_3$ crystals favour coarse-grained soil cementation, while smaller $CaCO_3$ crystals are more conducive to fine-grained soil biocementation of the treated soils (Tang et al., 2020).

By comparison, based on this study, *B. cereus* precipitated much smaller $CaCO_3$ crystals of 2.0–8.0 µm in diameter (Figure 6 a-c) than *B. paramycoides* which precipitated larger $CaCO_3$ crystals of 4.6–23.0 µm in diameter (Figure 6 e-f). Notably, the texture of organic and sandy clay soil treated in this study is silky and fine, therefore more favourable to biocementation with smaller $CaCO_3$ crystals. It is because fine-grained sands have smaller intergranular distances and more intergranular contacts. Hence, most of the smaller $CaCO_3$ coats the contact points, which could eventually enhance the overall cementation efficiency (Tang et al., 2020). It also might have further favoured *B. cereus*'s visible bio-cementation effect (Figure 7) over *B. paramycoides* because *B. cereus* precipitated much smaller $CaCO_3$ crystals. A detailed future study on factors influencing soil biocementation should be conducted to clarify the discrepancy in calcite crystal biocementation potential.

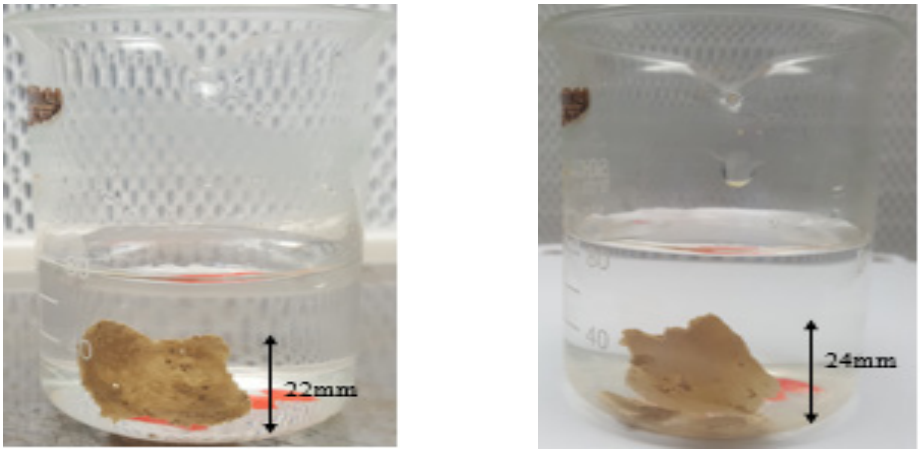

(a) (b)

Figure 7. Biocementation of soil samples treated by *Bacillus cereus* (a) sandy clay soil and (b) organic soil

The SEM-XRD microstructural analysis confirmed the deposition of bio-precipitated $CaCO_3$ on the treated soil grains by both bacterial species. The microstructural analysis of untreated soil samples (Figure 8 a and b) showed that the particle surfaces were smooth and distributed with large pores. By comparison, the inter-particle voids of all treated soil samples in Figure 8 (c, d, e, f) were densely filled and cemented by precipitated $CaCO_3$. SEM images of the treated soil samples in Figure 8f with only urea-calcium chloride medium showed particles surrounded with $CaCO_3$ even though the soil was not treated with any ureolytic bacteria under study.

XRD results of untreated soil showed characteristic diffraction peaks at 24.9°, 26.86°, 50.34°, 60.12° and 62.62° identified as defernite crystalline minerals which may be found in soil (Figure 9a) (Taner & Martin, 2013). The current study confirmed no $CaCO_3$ crystals in the untreated soil sample. Furthermore, the XRD results of treated soil samples with only urea-calcium chloride medium showed (Figure 9b) 2theta diffraction angles of 24.9°, 26.7°, 50.2° and 55.0°, which were attributed to defernite mineral. In comparison, distinct peaks at 20.9° and 62.3° were identified as vaterite and calcite, respectively. The abundant defernite minerals observed are part of the natural soil composition, as similarly observed in the untreated soil sample (Figure 9a), while the few calcite and vaterite crystals found may have been precipitated by the soil indigenous ureolytic bacteria since no $CaCO_3$ was introduced into the medium throughout the incubation period.

It is contrary to the study by Bibi et al. (2018), who reported no crystals or amorphous calcium carbonate precipitated after 30 days of incubation with only urea-calcium chloride medium on sampled soil from the Qatar desert. However, the present findings were expected as the sampled soils were urea-rich due to the frequent application of synthetic urea and organic manure during crop cultivation. Hence, such soils favour biodiversity and abundant distribution of *in situ* ureolytic bacteria (Zhu & Dittrich, 2016).

The microstructural analysis of sandy clay soil treated with *B. cereus* and *B. paramycoides* (Figure 8 c-f) showed pore spaces of soil grains surrounded by $CaCO_3$. The morphology of individual $CaCO_3$ crystals was not visible due to the dense formation of $CaCO_3$ clusters. However, the distribution of $CaCO_3$ bonds was qualitatively visualised, covering soil grains and forming bridges between grains. It is similar to the findings utilising pure cultures such as *B. licheniformis* (Helmi et al., 2016), *S. pasteurii* (Liu et al., 2021), *B. subtilis*, *S. pasteurii* and *B. sphaericus* (Sharma et al., 2021). The XRD spectra of *B. cereus* treated sandy clay soil (Figure 9c) showed distinct peaks at 29.6°, 36.1°, 39.6°, 48.7°, 57.6° and 61.0° attributed to calcite abundantly precipitated with some aragonite identified at 2theta diffraction angle of 43.4° in addition to peaks at 23.2°, 26.8° and 47.7° attributed to defernite crystals believed present in the soil. Furthermore, *B. paramycoides* treated sandy clay soil (Figure 9d) showed characteristic diffraction peaks at an angle of 29.4°, 36.0°, 39.4°, 43.1°, 48.4° and 57.4° revealing that the most precipitated bio-product

was calcite. In comparison, the only 2theta diffraction angle of 47.5° was identified as scawtite, a carbonised calcium silicate hydrate crystalline mineral believed to be in the soil (Grice, 2005).

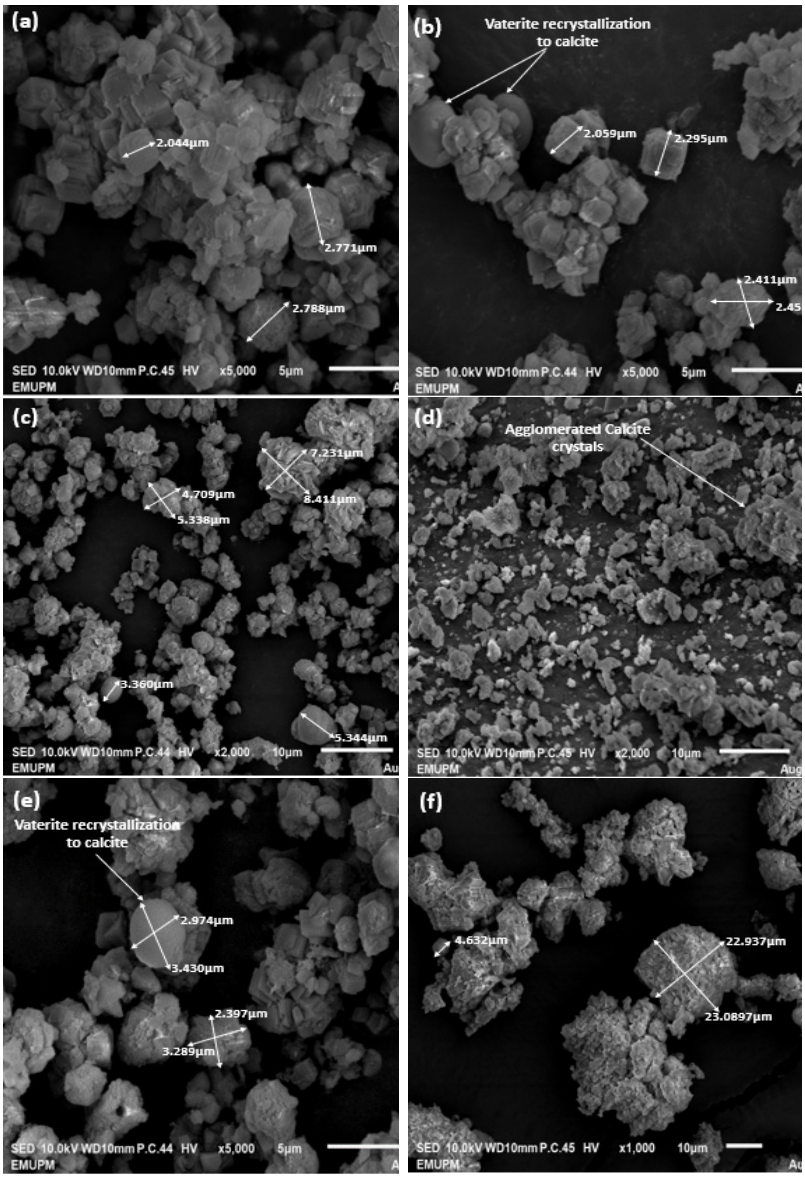

Figure 8. SEM micrographs of untreated/treated soil samples after 30 days of incubation at 28˚C ± 0.5°C. (a) Untreated sandy clay soil sample, (b) Treated sandy clay soil by *Bacillus cereus*, (c) Treated sandy clay soil by *Bacillus paramycoides*, (d) Treated organic soil by *Bacillus cereus,* (e) Treated organic soil by *Bacillus paramycoides,* and (f) Treated soil sample with urea–calcium chloride medium only.

Figure 8 (b, c, d & e) shows the SEM images of biocemented organic soil treated with *B. cereus* and *B. paramycoides*, respectively, with bio-precipitated $CaCO_3$ on the surfaces and contact points of soil particles. The $CaCO_3$ crystals were integrated tightly around the entire soil grain structure, with a decreased distance between the grains. Duo et al. (2018) found that the $CaCO_3$ crystals between soil particles improved the strength, enhanced the bearing capacity and reduced the permeability of the soil structure. The XRD spectra (Figure 9e) confirmed calcite to be the most abundant precipitated $CaCO_3$ polymorph by *B. cereus* with distinct peaks at 29.6°, 36.1°, 39.6°, 48.6°, 57.6° and 61.0°, with aragonite identified at peak 43.3°, in addition to peaks at 23.2°, 26.7° and 47.6° attributed to defernite. *B. paramycoides* precipitated calcite most at 2theta diffraction angles of 29.8°, 39.8° and 43.5°, while vaterite and aragonite were identified at 27.0°, 61.4° and 36.3°, 48.9° respectively in addition to scawtite at a diffraction angle of 23.5°, 47.8° and 57.8° (Figure 9f).

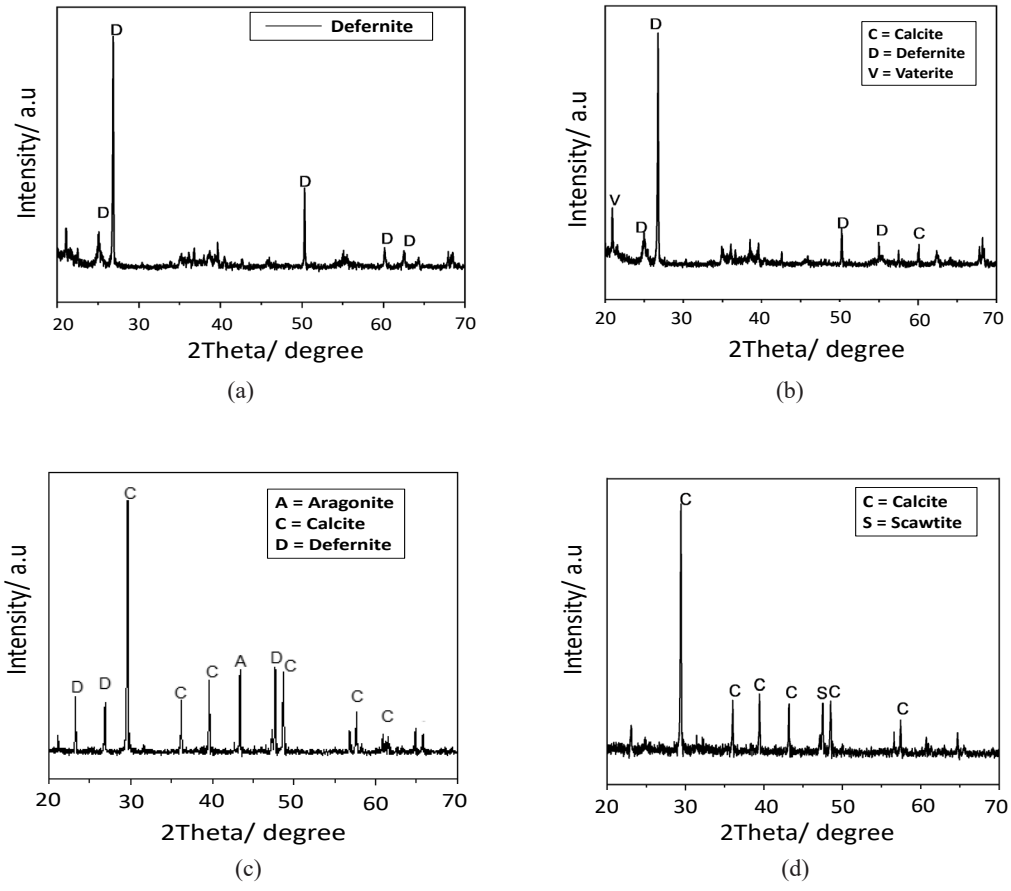

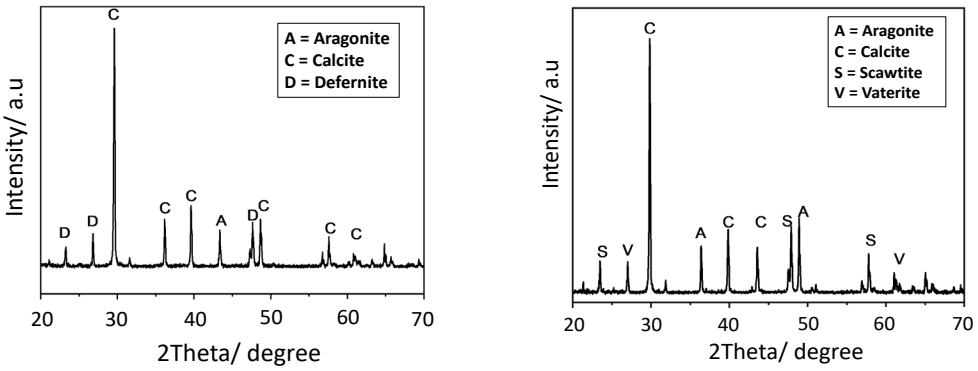

(e) (f)

Figure 9. XRD spectra of (a) Untreated soil sample, (b) Treated soil sample with Urea + $CaCl_2.2H_2O$, (c) Treated sandy clay soil sample by *B. cereus*, (d) Treated sandy clay soil sample by *B. paramycoides*, (e) Treated organic soil sample by *B. cereus*, (f) Treated organic soil sample by *B. paramycoides*

In the present study, all three polymorphic forms of crystalline $CaCO_3$ (calcite, vaterite and aragonite) were precipitated, with calcite being the most abundant $CaCO_3$ polymorph deposited onto the soil grains by both *B. cereus* and *B. paramycoides*, followed by vaterite and aragonite. Of note, vaterite is not naturally abundant but is an important precursor in calcite formation (Mwandira et al., 2017). Meanwhile, *B. cereus* precipitated more calcite than *B. paramycoides* in all treatments in this study. Consistent with our findings, most studies conducted through ureolysis-driven MICP confirmed calcite and vaterite crystalline polymorphic forms as the most precipitated (Al-Thawadi & Cord-Ruwisch, 2012; Algaifi et al., 2020). Calcite is the most preferable in MICP as it is the most thermodynamically stable polymorph (Chang et al., 2017). The solubility of $CaCO_3$ polymorphs increases in the order of calcite, aragonite, vaterite and amorphous calcium carbonate (Chang et al., 2017). Therefore, the lower solubility of aragonite and vaterite makes it difficult to obtain these polymorphs (Oral & Ercan, 2018). The characteristics mentioned above-favoured calcite over other $CaCO_3$ polymorphs in MICP for an effective soil stabilisation method. Although little is known with regard to what causes the bacterial precipitation of a particular polymorphic form of $CaCO_3$, previous investigations have shown that the selective precipitation of a specific polymorphic form is influenced by complex processes governed by several biotic and abiotic factors ranging from pH, urease enzyme specific amino acid sequence, medium composition to bacterial extracellular polymeric substances (Wei et al., 2015).

The calcite crystals observed in this study as the most precipitated polymorphic form of $CaCO_3$ in all treatments with *B. cereus* and *B. paramycoides* agreed with numerous studies (Bang et al., 2010; Achal et al., 2013). However, studies by Akyol et al. (2017) reported vaterite as the most precipitated form of $CaCO_3$, while Zhang et al. (2019) reported

aragonite as the most precipitated. Other polymorphic forms of bio-precipitated calcium carbonate include amorphous calcium carbonate and two hydrated crystalline phases: hexahydrocalcite ($CaCO_3.6H_2O$) and monohydrocalcite ($CaCO_3.H_2O$) (Anitha et al., 2018). Therefore, future comprehensive investigation of the parameters determining the formation of the polymorphic forms of $CaCO_3$ should be conducted.

In all cases, $CaCO_3$ mineral formation was bacteria associated, as none of the cultures had introduced $CaCO_3$ sources, and no mineral formation was detected in a medium without bacteria. Hence, the dynamic process of MICP leading to $CaCO_3$ precipitation is not chemically induced but microbially induced and directly linked with urea hydrolysis by bacterial urease activity (Alonso et al., 2018; Badiee et al., 2019; Osinubi et al., 2019).

CONCLUSION

B. cereus and *B. paramycoides* demonstrated high urease activity and precipitated large amounts of $CaCO_3$, including the three polymorphic forms of calcite, vaterite and aragonite. Since it is the most thermodynamically stable polymorph, calcite crystals were the most precipitated and preferable in MICP. Applying *B. cereus* and *B. paramycoides* to treat both organic and sandy clay soils results in the dense formation of $CaCO_3$ biocementing soil grains and filling inter-particle voids. Of note, *B. cereus* recorded the highest urease activity and precipitated more calcite with a better biocementing effect than *B. paramycoides*. Therefore, *B. cereus* is the preferred MICP bacterial candidate with the highest potential to be utilised as an agent for soil bio-stabilisation. This study established the presence of active indigenous urease $CaCO_3$ precipitating bacteria within the soil and their promising potential application as potential MICP agents for soil stabilisation.

ACKNOWLEDGEMENT

This work was financially supported by Universiti Putra Malaysia through Geran Universiti Putra Malaysia (Grant No: GP-IPS/2020/9691000). The authors express their appreciation for the support of all the laboratory science officers of the Faculty of Science, Universiti Putra Malaysia, for providing all the necessary assistance.

REFERENCES

Achal, V., Mukerjee, A., & Reddy, M. S. (2013). Biogenic treatment improves the durability and remediates the cracks of concrete structures. *Construction and Building Materials*, *48*, 1-5. https://doi.org/10.1016/j.conbuildmat.2013.06.061

Akyol, E., Bozkaya, O., & Dogan, N. M. (2017). Strengthening sandy soils by microbial methods. *Arab Journal of Geoscience*, *10*, Article 327. https://doi.org/10.1007/s12517-017-3123-9

Algaifi, H. A., Sam, A. R. M., Bakar, S. A., Abidin, R. Z., & Shahir, S. (2020). Screening of native ureolytic bacteria for self-healing in cementitious materials. In *IOP Conference Series: Material Science and Engineering* (Vol. 849, pp. 1-8). IOP Publishing. https://doi.org/10.1088/1757-899X/849/1/012074

Alonso, M. J. C., Ortiz, C. E. L., Perez, S. O. G., Narayanasamy, R., Miguel, G. D. J. F. S., Hernández, H. H., & Balagurusamy, N. (2018). Improved strength and durability of concrete through metabolic activity of ureolytic bacteria. *Environmental Science and Pollution Research*, *25*, 21451-21458. https://doi.org/10.1007/s11356-017-9347-0

Al-Thawadi, S., & Cord-Ruwisch, R. (2012). Calcium carbonate crystals formation by ureolytic bacteria isolated from Australian soil and sludge. *Journal of Advanced Science and Engineering Research*, *2*, 12-26.

Anitha, V., Abinaya, K., Prakash, S., Rao, A. S., & Vanavil, B. (2018). *Bacillus cereus* KLUVAA mediated biocement production using hard water and urea. *Chemical and Biochemical Engineering Quarterly*, *32*(2), 257-266. https://doi.org/10.15255/CABEQ.2017.1096

Badiee, H., Sabermahani, M., Tabandeh, F., & Javadi, A. S. (2019). Application of an indigenous bacterium in comparison with *Sporosarcina pasteurii* for improvement of fine granular soil. *International Journal of Environmental Science and Technology*, *16*(12), 8389-8400. https://doi.org/10.1007/s13762-019-02292-9

Bang, S. S., Galinat, J. K., & Ramakrishnan, V. (2001). Calcite precipitation induced by polyurethane-immobilized *Bacillus pasteurii*. *Enzyme and Microbial Technology*, *28*(4–5), 404–409. https://doi.org/10.1016/S0141-0229(00)00348-3

Bang, S. S., Lippert, J. J., Yerra, U., & Mulukutla, S. (2010). Microbial calcite, a bio-based smart nanomaterial in concrete remediation. *International Journal of Smart and Nano Materials*, *1*(1), 28-39. https://doi.org/10.1080/19475411003593451

Bernardi, D., Dejong, J. T., Montoya, B. M., & Martinez, B. C. (2014). Bio-bricks: Biologically cemented sandstone bricks. *Construction and Building Materials*, *55*, 462-469. https://doi.org/10.1016/j.conbuildmat.2014.01.019

Bibi, S., Oualha, M., Ashfaq, M. Y., Suleiman, M. T., & Zouari, N. (2018). Isolation, differentiation and biodiversity of ureolytic bacteria of Qatari soil and their potential in microbially induced calcite precipitation (MICP) for soil stabilization. *RSC Advances*, *8*(11), 5854-5863. https://doi.org/10.1039/C7RA12758H

Bzura, J., & Koncki, R. (2019). A mechanized urease activity assay. *Enzyme and Microbial Technology*, *123*, 1-7. https://doi.org/10.1016/j.enzmictec.2019.01.001

Chahal, N., Rajor, A., & Siddique, R. (2011). Calcium carbonate precipitation by different bacterial strains. *African Journal of Biotechnology*, *10*(42), 8359-8372. https://doi.org/10.5897/ajb11.345

Chang, I., Im, J., & Cho, G. C. (2016). Introduction of microbial biopolymers in soil treatment for future environmentally-friendly and sustainable geotechnical engineering. *Sustainability*, *8*(3), Article 251. https://doi.org/10.3390/su8030251

Chang, R., Kim, S., Lee, S., Choi, S., Kim, M., & Park, Y. (2017). Calcium carbonate precipitation for CO2 storage and utilization: A Review of the carbonate crystallization and polymorphism. *Frontiers in Energy Research*, *5*, Article 17. https://doi.org/10.3389/fenrg.2017.00017

Cheng, L., Shahin, M. A., & Cord-Ruwisch, R. (2014). Bio-cementation of sandy soil using microbially induced carbonate precipitation for marine environments. *Geotechnique*, *64*(12), 1010-1013. https://doi.org/10.1680/geot.14.T.025

Choi, S. G., Wang, K., Wen, Z., & Chu, J. (2017). Mortar crack repair using microbial induced calcite precipitation method. *Cement and Concrete Composites*, *83*, 209-221. https://doi.org/10.1016/j.cemconcomp.2017.07.013

Cizer, O., Van Balen, K., Elsen, J., & Van Gemert, D. (2008). Crystal morphology of precipitated calcite crystals from accelerated carbonation of lime binders. In *2nd International Conference on Accelerated Carbonation for Environmental and Materials Engineering* (ACEME08) (pp. 149-158). University of Rome.

Dadda, A., Geindreau, C., Emeriault, F., du Roscoat, S. R., Filet, A. E., & Garandet, A. (2018). Characterization of contact properties in biocemented sand using 3D X-ray micro-tomography. *Acta Geotechnica*, *14*, 597-613. https://doi.org/10.1007/s11440-018-0744-4

Dardau, A. A., Mustafa, M., & Abdaziz, N. A. (2021). Microbial-induced calcite precipitation: A milestone towards soil improvement. *Malaysian Applied Biology Journal*, *50*(1), 11-27. https://doi.org/10.55230/mabjournal.v50i1.8

Dhami, K. N., Mukherjee, A., & Reddy, M. S. (2016). Micrographical , minerological and nano-mechanical characterisation of microbial carbonates from urease and carbonic anhydrase producing bacteria. *Ecological Engineering*, *94*, 443-454. https://doi.org/10.1016/j.ecoleng.2016.06.013

Dhami, N. K., Reddy, M. S., & Mukherjee, M. S. (2013). Biomineralization of calcium carbonates and their engineered applications: A review. *Frontiers in Microbiology*, *4*, 314-327. https://doi.org/10.3389/fmicb.2013.00314

Filet, A. E., Gutjahr, I., Garandet, A., Viglino, A., Béguin, R., Sibourg, O., Monier, J. M., Martins, J., Oxarango, L., Spadini, L., Geindreau, C., Emeriault F., & Perthuisot, S. C. (2020). BOREAL, Bio-reinforcement of embankments by biocalcification. In *E3S Web of Conferences* (Vol. 195, p. 05001). EDP Sciences.. https://doi.org/10.1051/e3sconf/202019505001

Ghosh, T., Bhaduri, S., Montemagno, C., & Kumar, A. (2019). *Sporosarcina pasteurii* can form nanoscale calcium carbonate crystals on cell surface. *Plos One*, *14*(1), Article e0210339. https://doi.org/10.1371/journal.pone.0210339

Grice, J. D. (2005). The structure of spurrite, tilleyite and scawtite, and relationships to other silicate-carbonate minerals. *The Canadian Mineralogist*, *43*(5), 1489-1500. https://doi.org/10.2113/gscanmin.43.5.1489

Helmi, F. M., Elmitwalli, H. R., Elnagdy, S. M., & El-Hagrassy, A. F. (2016). Calcium carbonate precipitation induced by ureolytic bacteria *Bacillus licheniformis*. *Ecological Engineering*, *90*, 367-371. https://doi.org/10.1016/j.ecoleng.2016.01.044

Hoang, T., Alleman, J., Cetin, B., Ikuma, K., & Choi, S. G. (2019). Sand and silty sand soil stabilization using bacterial enzyme induced calcite precipitation (BEICP). *Canadian Geotechnical Journal*, *56*(6), 808-822. https://doi.org/10.1139/cgj-2018-0191

Imran, M. A., Kimura, S., Nakashima, K., Evelpidou, N., & Kawasaki, S. (2019). Feasibility study of native ureolytic bacteria for biocementation towards coastal erosion protection by MICP method. *Applied Sciences*, *9*(20), Article 4462. https://doi.org/10.3390/app9204462

Ivanov, V., Stabnikov, V., Stabnikova, O., & Ahmed, Z. (2020). Biocementation technology for construction of artificial oasis in sandy desert. *Journal of King Saud University - Engineering Sciences*, *32*(8), 491-494. https://doi.org/10.1016/j.jksues.2019.07.003

Jiang, N. J, Tang, C. S, Hata, T., Courcelles, B., Dawoud, O., & Singh, D. N. (2020). Bio-mediated soil improvement: The way forward. *Soil Use and Management*, *36*(2), 185-188. https://doi.org/10.1111/sum.12571

Jiang, N. J., Yoshioka, H., Yamamoto, K., & Soga, K. (2016). Ureolytic activities of a urease-producing bacterium and purified urease enzyme in the anoxic condition: Implication for subseafloor sand production control by microbially induced carbonate precipitation (MICP). *Ecological Engineering*, *90*, 96-104. https://doi.org/10.1016/j.ecoleng.2016.01.073

Kakelar, M. M., Ebrahimi, S., & Hosseini, M. (2016). Improvement in soil grouting by biocementation through injection method. *Asia-Pacific Journal of Chemical Engineering*, *11*(6), 930-938. https://doi.org/10.1002/apj.2027

Keykha, H. A., Asadi, A., & Zareian, M. (2017). Environmental factors affecting the compressive strength of microbiologically induced calcite precipitation treated soil. *Geomicrobiology Journal*, *34*(10), 889-894. https://doi.org/10.1080/01490451.2017.1291772

Kim, G., & Youn, H. (2016). Microbially induced calcite precipitation employing environmental isolates. *Materials*, *9*(6), Article 468. https://doi.org/10.3390/ma9060468

Kim, G., Kim, J., & Youn, H. (2018). Effect of temperature , pH , and reaction duration on microbially induced calcite precipitation. *Applied Sciences*, *8*(8), Article 1277. https://doi.org/10.3390/app8081277

Kim, J. H., & Lee, J. Y. (2019). An optimum condition of MICP indigenous bacteria with contaminated wastes of heavy metal. *Journal of Material Cycles and Waste Management*, *21*, 239-247. https://doi.org/10.1007/s10163-018-0779-5

Li, D., Tian, K. L., Zhang, H. L., Wu, Y. Y., Nie, K. Y., & Zhang, S. C. (2018). Experimental investigation of solidifying desert aeolian sand using microbially induced calcite precipitation. *Construction and Building Materials*, *172*, 251-262. https://doi.org/10.1016/j.conbuildmat.2018.03.255

Li, M., Fu, Q. L., Zhang, Q., Achal, V., & Kawasaki, S. (2015). Bio-grout based on microbially induced sand solidification by means of asparaginase activity. *Scientific Reports*, *5*, Article 16128. https://doi.org/10.1038/srep16128

Liu, B., Xie, Y. H., Tang, C. S., Pan, X. H., Jiang, N. J., Singh, D. N., Cheng, Y. J., & Shi, B. (2021). Bio-mediated method for improving surface erosion resistance of clayey soils. *Engineering Geology*, *293*, Article 106295. https://doi.org/10.1016/j.enggeo.2021.106295

Liu, Y., Chen, Y., Huang, X., & Wu, G. (2017). Biomimetic synthesis of calcium carbonate with different morphologies and polymorphs in the presence of bovine serum albumin and soluble starch. *Materials Science and Engineering: C*, *79*, 457–464. https://doi.org/10.1016/j.msec.2017.05.085

Luo, M., & Qian, C. X. (2016). Performance of two bacteria-based additives used for self-healing concrete. *Journal of Materials in Civil Engineering*, *28*(12), Article 04016151. https://doi.org/10.1061/(asce)mt.1943-5533.0001673

Makinda, J., Gungat, L., Rao, N. S. V. K., & Sulis, S. (2018). Compressibility behaviour of Borneo tropical peat stabilized with lime-sand column. *International Journal on Advanced Science, Engineering and Information Technology*, *8*(1), 172-177. https://doi.org/10.18517/ijaseit.8.1.4169

Miftah, A., Tirkolaei, H. K., & Bilsel, H. (2020). Biocementation of calcareous beach sand using enzymatic calcium carbonate precipitation. *Crystals*, *10*(10), Article 888. https://doi.org/10.3390/cryst10100888

Morsdorf, G., & Kaltwasser, H. (1989). Ammonium assimilation in *Proteus vulgaris*, *Bacillus pasteurii*, and *Sporosarcina ureae*. *Archives of Microbiology*. *152*, 125-131. https://doi.org/10.1007/BF00456089

Mortensen, B. M., Haber, M. J., Dejong, J. T., Caslake, L. F., & Nelson, D. C. (2011). Effects of environmental factors on microbial induced calcium carbonate precipitation. *Journal of Applied Microbiology*, *111*(2), 338-349. https://doi.org/10.1111/j.1365-2672.2011.05065.x

Muthukkumaran, K., & Shashank, B. S. (2016). Durability of microbially induced calcite precipitation (MICP) treated cohesionless soils. *Japanese Geotechnical Society Special Publication*, *2*(56), 1946-1949. https://doi.org/10.3208/jgssp.IND-23

Mwandira, W., Nakashima, K., & Kawasaki, S. (2017). Bioremediation of lead-contaminated mine waste by *Pararhodobacter* sp. based on the microbially induced calcium carbonate precipitation technique and its effects on strength of coarse and fine grained sand. *Ecological Engineering*, *109*(Pt. A), 57-64. https://doi.org/10.1016/j.ecoleng.2017.09.011

Mwandira, W., Nakashima, K., Kawasaki, S., Ito, M., Sato, T., Igarashi, T., Chirwa, M., Banda, K., Nyambe, I., Nakayama, S., Nakata, H., & Ishizuka, M. (2019). Solidification of sand by Pb(II)-tolerant bacteria for capping mine waste to control metallic dust: Case of the abandoned Kabwe Mine, Zambia. *Chemosphere*, *228*, 17-25. https://doi.org/10.1016/j.chemosphere.2019.04.107

Nawarathna, T. H. K., Nakashima, K., & Kawasaki, S. (2018). Enhancement of microbially induced carbonate precipitation using organic biopolymer. *International Journal of Geomate*, *14*(41), 7-12. https://doi.org/10.21660/2018.41.7223

Nawarathna, T. H. K., Nakashima, K., & Kawasaki, S. (2019). Chitosan enhances calcium carbonate precipitation and solidification mediated by bacteria. *International Journal of Biological Macromolecules*, *133*, 867-874. https://doi.org/10.1016/j.ijbiomac.2019.04.172

Nething, C., Smirnova, M., Gröning, J. A. D., Haase, W., Stolz, A., & Sobek, W. (2020). A method for 3D printing bio-cemented spatial structures using sand and urease active calcium carbonate powder. *Materials and Design*, *195*, Article 109032. https://doi.org/10.1016/j.matdes.2020.109032

Omoregie, A. I., Ngu, L. H., Ong, D. E. L., & Nissom, P. M. (2019). Low-cost cultivation of *Sporosarcina pasteurii* strain in food-grade yeast extract medium for microbially induced carbonate precipitation (MICP) application. *Biocatalysis and Agricultural Biotechnology*, *17*, 247-255. https://doi.org/10.1016/j.bcab.2018.11.030

Omoregie, A., Khoshdelnezamiha, G., Ong, D. E. L., & Nissom, P. M. (2017). Microbial-induced carbonate precipitation using a sustainable treatment technique. *International Journal of Service Management and Sustainability*, *2*(1), 17-31. http://dx.doi.org/10.24191/ijsms.v2i1.6045

Oral, Ç. M., & Ercan, B. (2018). Influence of pH on morphology, size and polymorph of room temperature synthesized calcium carbonate particles. *Powder Technology*, *339*, 781-788. https://doi.org/10.1016/j.powtec.2018.08.066

Oshiki, M., Araki, M., Hirakata, Y., Hatamoto, M., Yamaguchi, T., & Araki, N. (2018). Ureolytic prokaryotes in soil: Community abundance and diversity. *Microbes and Environments*, *33*(2), 230-233. https://doi.org/10.1264/jsme2.ME17188

Osinubi, K. J., Eberemu, A. O., Gadzama, E. W., & Ijimdiya, T. S. (2019). Plasticity characteristics of lateritic soil treated with *Sporosarcina pasteurii* in microbial-induced calcite precipitation application. *SN Applied Sciences*, *1*, Article 829. https://doi.org/10.1007/s42452-019-0868-7

Pablo, A. C. M. S., Lee, M, Graddy, C. M. R., Kolbus, C. M., Khan, M., Zamani, A., Martin, N., Acuff, C., Dejong, J. T., Gomez, M. G., & Nelson, D. C. (2020). Meter-scale biocementation experiments to advance process control and reduce impacts: Examining spatial control, ammonium by-product removal, and chemical reductions. *Journal of Geotechnical and Geoenvironmental Engineering*, *146*(11), 1-14. https://doi.org/10.1061/(ASCE)GT.1943-5606.0002377

Park, S. J., Park, Y. M., Chun, W. Y., Kim, W. J., & Ghim, S. Y. (2010). Calcite-forming bacteria for compressive strength improvement in mortar. *Journal of Microbiology and Biotechnology*, *20*(4), 782-788.

Qabany, A. A., Soga, K., & Santamarina, C. (2011). Factors affecting efficiency of microbially induced calcite precipitation. *Journal of Geotechnical and Geoenvironmental Engineering*, *138*(8), 992-1001. https://doi.org/10.1061/(asce)gt.1943-5606.0000666

Rabenhorst, M., Buchanan, A., Morozov, E., Shay, J., & Mack, S. (2020). Field test for identifying problematic red parent materials. *Soil Science Society of American Journal*, *84*(3), 1006-1010. https://doi.org/10.1002/saj2.20066

Renner, L. D., & Weibel, D. B. (2011). Physicochemical regulation of biofilm formation. *MRS Bulletin*, *36*, 347-355. https://doi.org/10.1557/mrs.2011.65

Richardson, A., Coventry, K. A., Forster, A. M., & Jamison, C. (2014). Surface consolidation of natural stone materials using microbial induced calcite precipitation. *Structural Survey*, *32*(3), 265-278. https://doi.org/10.1108/SS-07-2013-0028

Ritchey, E. L., McGrath, J. M., & Gehring, D. (2015). *Determining soil texture by feel*. Agriculture and Natural Resources Publications.

Sapar, N. I. F., Matlan, S. J., Mohamad, H. M., Alias, R., & Ibrahim, A. (2020). A study on physical and morphological characteristics of tropical peat in Sabah. *International Journal of Advanced Research in Engineering and Technology (IJARET)*, *11*(11), 542-553.

Sharma, M., Satyam, N., & Reddy, K. R. (2021). Investigation of various gram-positive bacteria for MICP in Narmada Sand, India. *International Journal of Geotechnical Engineering*, *15*(2), 220-234. https://doi.org/10.1080/19386362.2019.1691322

Singh, M. J., Weiqiang, F., Dong-Sheng, X., & Borana, L. (2020). Experimental study of compression behavior of Indian black cotton soil in oedometer condition. *International Journal of Geosynthetics and Ground Engineering*, *6*, Article 30. https://doi.org/10.1007/s40891-020-00207-0

Sinha, S., & Chattopadhyay. S. (2016). A study on application of renewable energy technologies for mitigatting the adverse environmental impacts generated from power generation units in Himalayan region. *International Journal for Innovative Research in Science & Technology*, *3*(1), 212-232.

Srivastava, S., Bharti, R. K., & Thakur, I. S. (2014). Characterization of bacteria isolated from palaeoproterozoic metasediments for sequestration of carbon dioxide and formation of calcium carbonate. *Environmental Science and Pollution Research*, *22*, 1499-1511. https://doi.org/10.1007/s11356-014-3442-2

Svane, S., Sigurdarson, J. J., Finkenwirth, F., Eitinger, T., & Karring, H. (2020). Inhibition of urease activity by different compounds provides insight into the modulation and association of bacterial nickel import and ureolysis. *Scientific Reports*, *10*, Article 8503. https://doi.org/10.1038/s41598-020-65107-9

Taner, F. M., Martin, R. F. & Gault, R. A. (2013). The mineralogy of skarns of the spurrite-merwinite subfacies, sanidinite facies, Guneyce-ikizdere area, eastern black sea, Turkey. *The Canadian Mineralogist*, *51*(6), 893-911. https://doi.org/10.3749/canmin.51.6.893

Tang, C. S., Yin, L. Y., Jiang, N. J., Zhu, C., Zeng, H., Li, H., & Shi, B. (2020). Factors affecting the performance of microbial-induced carbonate precipitation (MICP) treated soil: A review. *Environmental Earth Sciences*, *79*, Article 94. https://doi.org/10.1007/s12665-020-8840-9

Terzis, D., & Laloui, L. (2019). Cell-free soil bio-cementation with strength, dilatancy and fabric characterization. *Acta Geotechnica*, *14*, 639-656. https://doi.org/10.1007/s11440-019-00764-3

Towner, G. D. (1974). The assessment of soil texture from soil strength measurements. *Journal of Soil Science*, *25*(3), 298-306. https://doi.org/10.1111/j.1365-2389.1974.tb01125.x

Wahab, N., Talib, M. K. A., & Rohani, M. M. (2019). An introduction of tropical peat and its history of shear strength in Malaysia. *International Journal of Civil Engineering and Technology (IJCIET)*, *10*(5), 695-705.

Wang, Z., Zhang, N., Cai, G., Jin, Y., Ding, N., & Shen, D. (2017). Review of ground improvement using microbial induced carbonate precipitation (MICP). *Marine Georesources and Geotechnology*, *35*(8), 1135-1146. https://doi.org/10.1080/1064119X.2017.1297877

Warren, L. A., Maurice, P. A., Parmar, N., & Ferris, F. G. (2001). Microbially mediated calcium carbonate precipitation: Implications for interpreting calcite precipitation and for solid-phase capture of inorganic contaminants. *Geomicrobiology Journal*, *18*(1), 93-115. https://doi.org/10.1080/01490450151079833

Wath, R. B., & Pusadkar, S. S. (2016). Soil improvement using microbial: A review. In T. Thyagaraj (Ed.), *Lecture Notes in Civil Engineering: Vol. 14. Ground Improvement Techniques and Geosynthetics* (pp. 329-335). Springer. https://doi.org/10.1007/978-981-13-0559-7_37

Wei, S., Cui, H., Jiang, Z., Hao, L., He, H., & Fang, N. (2015). Biomineralization processes of calcite induced by bacteria isolated from marine sediments. *Brazilian Journal of Microbiology*, *46*(2), 455-464. https://doi.org/10.1590%2FS1517-838246220140533

Wen, K., Li, Y., Amini, F., & Li, L. (2020). Impact of bacteria and urease concentration on precipitation kinetics and crystal morphology of calcium carbonate. *Acta Geotechnica*, *15*, 17-27. https://doi.org/10.1007/s11440-019-00899-3

Wiley, W. R., & Stokes, J. L. (1963). Effect of pH and ammonium ions on the permeability of *Bacillus pasteurii*. *Journal of Bacteriology*, *86*, 1152-1156. https://doi.org/10.1128/jb.86.6.1152-1156.1963

Wong, L. S. (2015). Microbial cementation of ureolytic bacteria from the genus Bacillus: A review of the bacterial application on cement based materials for cleaner production. *Journal of Cleaner Production*, *93*, 5-17. https://doi.org/10.1016/j.jclepro.2015.01.019

Wu, J., Wang, X. B., Wang, H. F., & Zeng, R. J. (2017). Microbially induced calcium carbonate precipitation driven by ureolysis to enhance oil recovery. *RSC Advances*, *7*(59), 37382-37391. https://doi.org/10.1039/c7ra05748b

Zhang, J., Zhao, C., Zhou, A., Yang, C., Zhao, L., & Li, Z. (2019). Aragonite formation induced by open cultures of microbial consortia to heal cracks in concrete: Insights into healing mechanisms and crystal polymorphs. *Construction and Building Materials*, *224*, 815-822. https://doi.org/10.1016/j.conbuildmat.2019.07.129

Zhu, T., & Dittrich, M. (2016). Carbonate precipitation through microbial activities in natural environment, and their potential in biotechnology: A review. *Frontiers in Bioengineering and Biotechnology*, *4*, Article 4. https://doi.org/10.3389/fbioe.2016.00004